Proceedings of Ninth World Conference on Earthquake Engineering
August 2-9, 1988, Tokyo-Kyoto, JAPAN (Vol.III)

4-2-5

# NONLINEAR DYNAMIC RESPONSE ANALYSIS BY THE DEFORMATION MODEL OF SOILS UNDER COMBINED STRESSES

Yoshiharu KIYOTA[1)], Akio HARA[1)], Yoshiroh SAKAI[2)] and Takayuki AOYAGI[3)]

[1] Kajima Institute of Construction Technology, Chofu-shi, Tokyo 182, Japan
[2] Tokyo Electric Power Company, Chofu-shi, Tokyo 182, Japan
[3] Tokyo Electric Power Services Co., LTD, Chiyoda-ku, Tokyo 100, Japan

SUMMARY

Concerning soil-structure interaction, a stress-strain model for soil under general stress conditions is required in order to evaluate the deformation in the soil. In the paper, "Deformation Model of Soils under Combined Stresses", a method is proposed for evaluating deformation when axial stress and shearing stress vary simultaneously.

The results from the shaking table tests with the model, in which extreme nonlinear phenomenan occurred, were analyzed using the proposed model. The results of analysis with the proposed model and test results agreed closely.

## INTRODUCTION

As shown in Fig. 1(a), stress conditions in one-dimensional soil deposits are nearly constant for vertical stress $\sigma_v$ and horizontal stress $\sigma_h$, and only the shear stress $\tau_{hv}$ varies. However, in layers adjacent to structures, $\sigma_v$, $\sigma_h$ and $\tau_{hv}$ change independently due to soil-structure interaction, as Fig. 1(b) shows. Because the dependency on confining pressure of soils is remarkable, a stress-strain model for soil under general stress conditions where $\sigma_v$, $\sigma_h$ and $\tau_{hv}$ vary simultaneously is required.

The authors propose a deformation model for soil under combined stresses. This model can express deformation of soil under general stress conditions. It was shown that the results of the tests and analysis agree closely in the range of static tests.[1)]

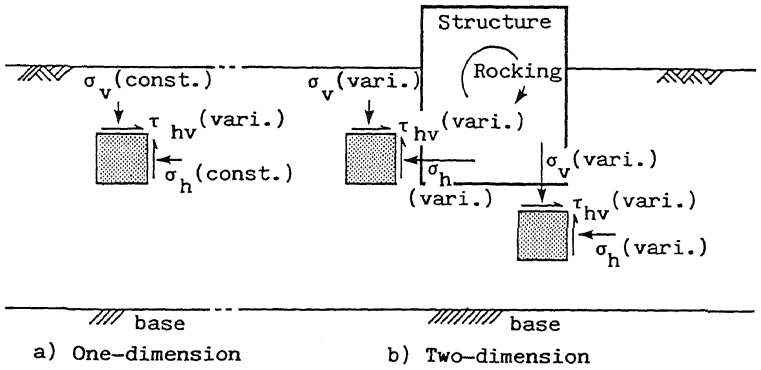


Fig. 1 Stress conditions in one and two-dimensional soil deposits

In order to confirm the validity of the proposed model by dynamic tests, analysis of model tests with a large shaking table was conducted. Moreover, a comparison was made of nonlinear analysis with the conventional analysis based on the equivalent linear method.

## PROPOSAL OF DEFORMATION MODEL

Concept of Model As shown in Fig.2, the shear modulus G of soil is usually expressed as the secant modulus. However, the stress-strain point on a hysteresis curve cannot be expressed by the secant modulus G. Therefore, the tangential shear modulus G* at any point is defined in this paper. The relationship between tangential shear modulus G* and shear stress $\tau$ can be expressed refering to Fig.3 as follows:

$$G^*/Go=f(|\tau/Su|) \qquad (1)$$

where, Go: Initial shear modulus; Su: Maximum shear strength.

In Fig.3 an elastic body follows the path from ① to ② , an elasto-plastic body from ① to ③ , and a rigid-Plastic body from ① to ② to ③ . In other words, the principles of elasticity, elasto-plasticity and rigid-plasticity of materials are represented in Fig.3.

Next, assuming the ralationship between G/Go and $\tau$/Su is continually changing, Eq.(1) becomes the following equation.

$$G^*/Go=(1-|\tau/Su|)^n \qquad (2)$$

The following equation is obtained when Eq.(2) is regarded as a differential equation involving shear stress and shear strain $\gamma$.

$$\gamma=\int_0^\tau \frac{1}{Go}\cdot\frac{1}{(1-|\tau/Su|)^n}\cdot d\tau \qquad (3)$$

If this is solved using the reference strain $\gamma f(=Su/Go)$ at n=2, the following equation is obtained.

$$\frac{\tau}{Su}=\frac{\gamma/\gamma_f}{1+|\gamma/\gamma_f|} \qquad (4)$$

This is proven to be a known H-D model. The parameters Go and Su in Eq.(4) are given by the following equations.

$$Go=a\left(\frac{\sigma_v+\sigma_h}{2}\right)^b \qquad (5)$$

$$Su=\frac{\sigma_v+\sigma_h}{2}\cdot\sin\phi \qquad (6)$$

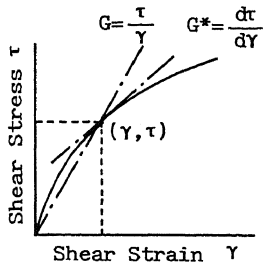


Fig. 2 Definition of G and G*

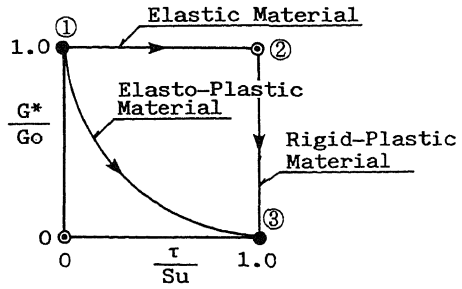


Fig. 3 Relationship between tangential shear modulus and shear stress including elastic, elasto-plastic and rigid-plastic materials

Simple Shear Test Under Various Overburden Pressure[2] In order to understand the dependence on overburden pressure of the deformation properties of soil, a series of simple shear tests were performed under various overburden pressures $\sigma_v$ . Table 1 shows the test conditions for samples within a narrow range of unit weight.

Test results of the ten samples numbered in Table 1 are shown in Fig.4. In this figure, the value of G at $\gamma$=0.0001% is regarded as the initial shear modulus Go. The relationship between G/Go and $\gamma$ is shown in Fig.5. From this figure, it can be seen that as $\sigma_v$ increases, G/Go shows a slight decrease, and the increase of h becomes slower.

Defining the shear strain at G/Go=0.5 to be the reference strain $\gamma_{0.5}$ , the relationships between G/Go and $\gamma/\gamma_{0.5}$ and between h and $\gamma/\gamma_{0.5}$ are shown in Fig.6. From this figure, it can be seen that the relationships between G/Go and $\gamma/\gamma_{0.5}$ and between h and $\gamma/\gamma_{0.5}$ are well-normalized curves. The broken line in Fig.6 shows the curve of the H-D model, but the values do not agree closely in the range $1.0 < \gamma/\gamma_{0.5}$ .

Table 1 Soil Properties and Test Conditions

| Test No. | Unit Weight $\gamma_t$ (g·f/cm ) | Vertical Stress $\sigma_v$ (kg·f/cm ) |
|---|---|---|
| 1 | 1.632 | 0.3 |
| 2 | 1.647 | 0.4 |
| 3 | 1.646 | 0.5 |
| 4 | 1.642 | 0.6 |
| 5 | 1.636 | 0.7 |
| 6 | 1.650 | 0.8 |
| 7 | 1.635 | 1.0 |
| 8 | 1.642 | 1.5 |
| 9 | 1.639 | 2.0 |
| 10 | 1.646 | 3.0 |

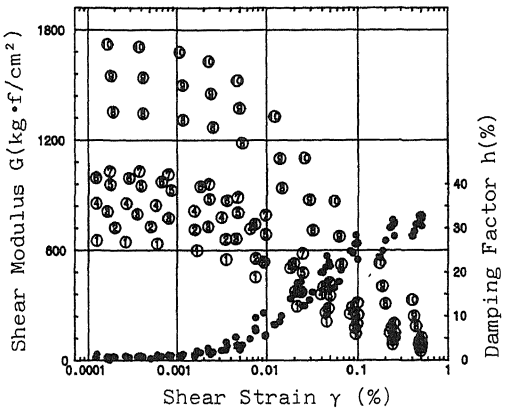

Fig. 4 G∿γ, h∿γ relationships

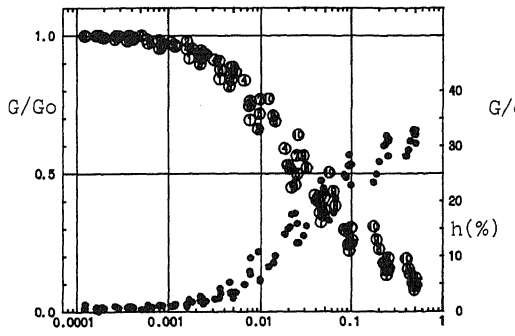

Fig. 5 G/Go∿γ, h∿γ relationships

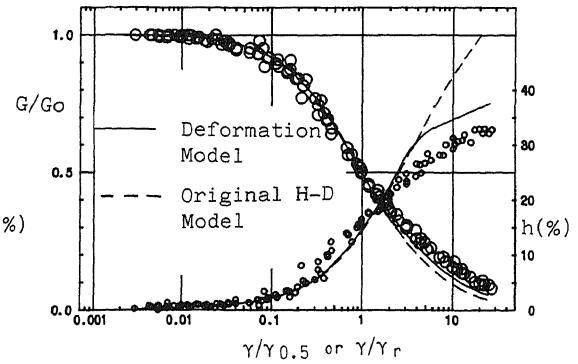

Fig. 6 G/Go∿γ/γr, h∿γ/γr relationships

Introduction of Reference Strength Under Stress Path As can be seen in Fig.6, the original H-D model is limited for describing the deformation properties of soil. Therefore, a reference shear strength $\tau_r$ and reference shear strain $\gamma_r$ satisfying the following conditions are introduced to the existing H-D model.

$$\gamma_r = \tau_r / Go \qquad (7)$$

$$|\tau| < \tau_r \leqq Su \qquad (8)$$

where, $|\tau| \to Su$, when $\tau_r \to Su$.

The actual $\tau_r$ is determined according to Fig.7. The types of stress path include the following three kinds:

i) When shear stress increases monotonously, it follows the path ⓪→Ⓕ ;

ii) When the direction of $\tau$ is reversed and it does not exceed the value of $\tau$/Su, it follows the path ⓪→①→②→③ ;

iii) When it receives a value of $\tau$ which exceeds the previous values of $\tau$/Su , it follows, for example, the path ⓪→①→②→③→④ .

In any case, the value $\tau_r/Su$ does not always decrease. As mentioned above, by introducing $\tau_r$ and $\gamma_r$ which take into account the stress path, the following equation is obtained which agrees with the H-D model given by Eq.(4) at failure.

$$\frac{\tau}{\tau_r}=\frac{\gamma/\gamma_r}{1+|\gamma/\gamma_r|} \qquad (9)$$

In Fig.6, the relationships $G/Go \sim \gamma/\gamma_r$ and $h \sim \gamma/\gamma_r$ obtained after considering the stress path are shown with a solid line. It can be seen that the solid line agrees well with the test results.

Application to FEM The tangential shear modulus G* at the time shear stress acts as an external force is given by the following equation.

$$G^*=Go\cdot(1-|\gamma/\gamma_r|)^2 \qquad (10)$$

When the normal stress ( $\sigma_v$ , $\sigma_h$ ) acts as an external force, the tangential Young's modulus E* is given by the following equation.

$$E^*=2(1+\nu)\cdot G^* \qquad (11)$$

The stiffness matrix of FEM can be produced using the values of E* and G* obtained from Eqs. (10) and (11) instead of using the given values of elastic modulus E and G.

The flow chart for the nonlinear response analysis program is given in Fig.8. As the figure shows, the stiffness matrix is generated at each step. Moreover, for the range of increasing load, convergent calculation is required until the stress and strain satisfy Eq.(9).

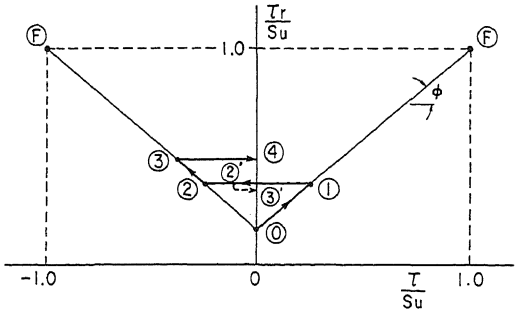


Fig. 7 Introduction of reference strength under stress path

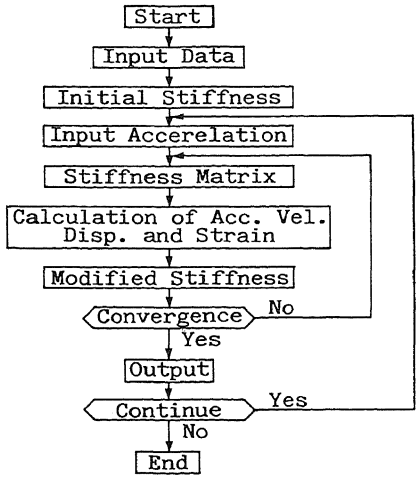


Fig. 8 Flow chart for FEM analysis

## COMPARISON WITH TEST RESULTS

Test procedures[3] Fig. 9(a, b) shows a section and plan of the model. The soil box and the building model are made of steel while the supporting ground is silicone rubber ($E=41kg\cdot f/cm^2$, $\nu=0.48$). The surface soil is backfilled with Toyoura sand. The tests were performed with a shaking table which applied the sweep waves shown in Fig. 10.

Analysis Fig. 11 shows the element mesh for FEM analysis. Using this element mesh, three types of analysis were conducted: analysis using the deformation model, equivalent linear analysis and linear analysis. For each type of analysis, the following input data were used.

$$Go=1000\sigma_v^{0.5},\ \phi=40^0,\ \nu=1/3 \qquad (12)$$

where the $G/GO \sim \gamma$ and $h \sim \gamma$ relationships required for the equivalent linear method were taken from Fig. 6. For the linear method, the value of shear modulus given by Eq. 12 was used.

Fig. 12 shows the response accelerations at the top of model structure for the tests, the deformation model, the equivalent linear method and the linear method.

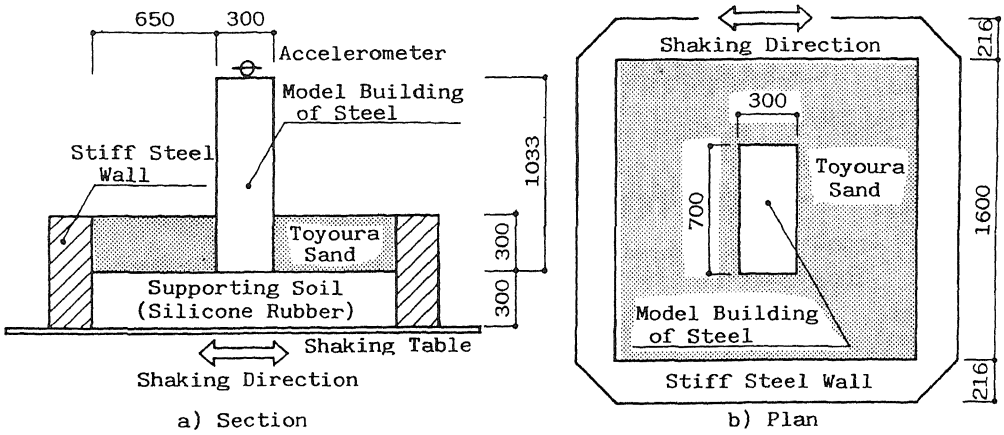


Fig. 9 Diagram of shaking table test.

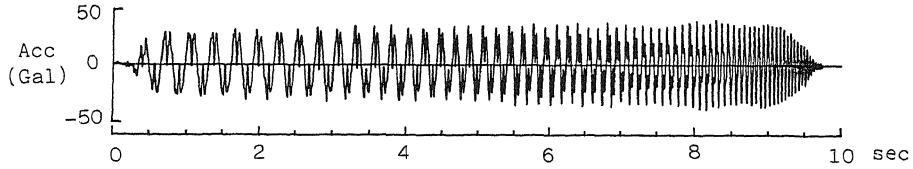


Fig. 10 Input wave

As can be seen from this figure, the deformation model agrees most closely with the test results, followed by the equivalent linear method. The agreement of the test results with the linear method is very low.

Fig. 13 shows the frequency transfer function between the shaking table and the top of the model building for the tests, for the deformation model and for the equivalent linear analysis. As can be seen from this figure, the period and amplitude of the rocking mode of the building model obtained from the tests and from analysis with the deformation model are indentical. However, the results obtained from equivalent linear analysis disagree greatly.

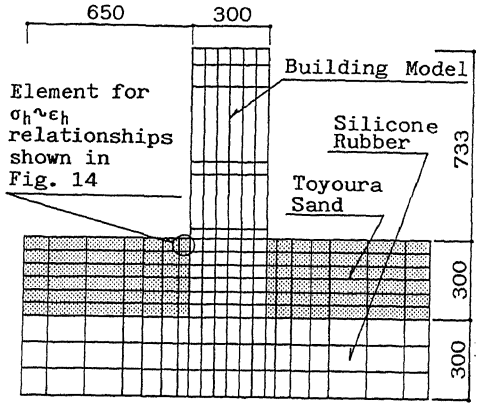


Fig. 11 Element mesh for FEM analysis

Fig. 14 shows hysteresis loops between the horizontal stress $\sigma_h$ and horizontal strain $\varepsilon_h$ for the elements directly in contact with the model building shown in Fig. 11. For these elements, the hysteresis curves are triangular and are affected by the rocking of the building. The extreme non-linearity of the soil results in an active state on some parts.

## CONCLUSIONS

1) The input data is simpler than any of the conventional methods of nonlinear analysis.
2) The assumption was made that reference shear strength depends on stress path. With this assumption, the relationships $G/Go \sim \gamma/\gamma_r$ and $h \sim \gamma/\gamma_r$ were closer to the test results than the existing H-D model.

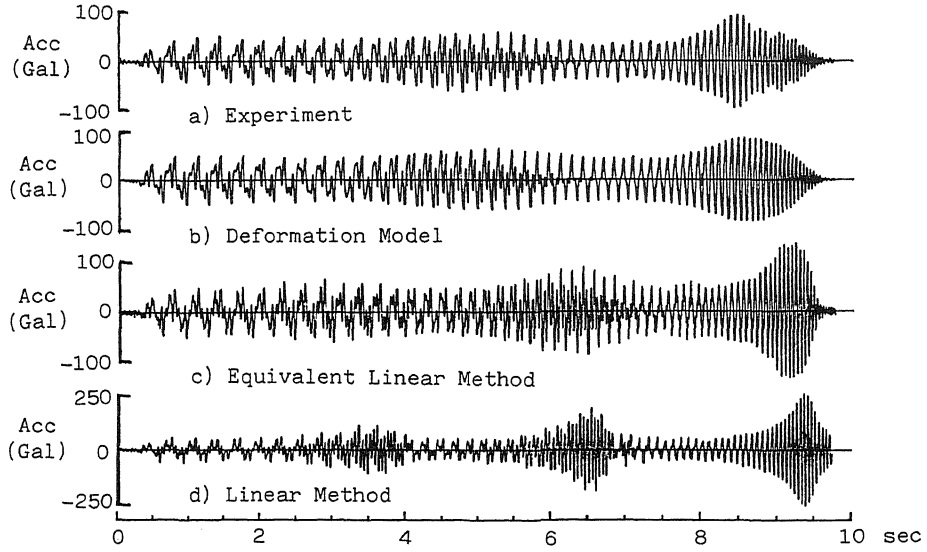


Fig. 12 Comparison of observed Acc. and computed Acc. at the top of model structure

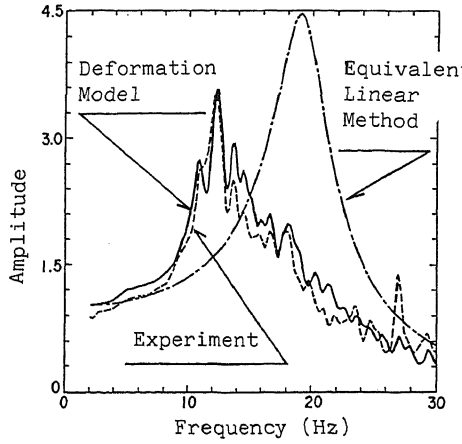


Fig. 13 Frequency transfer function between the shaking table and the top of the model building

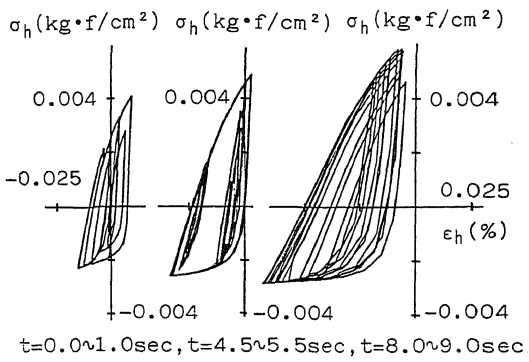


Fig. 14 Hysteresis curves of soil element shown in Fig. 11

3) For tests with remarkable nonlinearity, such as in this paper, simulation with the conventional equivalent linear method is of limited accuracy. The results of analysis based on the proposed method in this study agreed quite closely with the test results.

## REFERENCES

1. Hara, A., Kiyota, Y., Sakai, Y., Aoyagi, T., "Experiments and Analysis for the Hysteresis Characteristics of Soil", 3rd ICSDEE, vol. 42, pp 337 - 342, (1987).
2. Hara, A., Kiyota, Y., "Dependency on Overburden Pressure of Deformation Properties of Soil" the 19th JNCSMFE, pp 235 - 236, (1984).
3. Yano, A., Hara, A., Naito, U., "Shaking Table Test and Analysis of Soil-Structure Interaction (Part 5 Examination of Dynamic Earth Pressure)" Sum. of tech. papers of ann. meet, A.I.J. pp 171 - 172, (1985).